ELSEVIER

Engineering Geology 59 (2001) 83–102

ENGINEERING GEOLOGY

www.elsevier.nl/locate/enggeo

Structural constraints on deep-seated slope deformation kinematics

F. Agliardi[a], G. Crosta[a,*], A. Zanchi[b]

[a]*Dipartimento di Scienze Geologiche e Geotecnologie, Università di Milano-Bicocca, Piazza della Scienza 4, 20126 Milan, Italy*
[b]*Dipartimento di Scienze dell'Ambiente e del Territorio, Università di Milano-Bicocca, Piazza della Scienza 1, 20126 Milan, Italy*

Received 2 February 2000; accepted for publication 29 June 2000

Abstract

A significant sackung-type deep-seated slope gravitational deformation (DSGSD) was recognised for the first time by the authors in the middle part of Valfurva, east of Bormio (Rhaetian Alps, Italy). The reconstruction of its kinematics, age and state of activity is presented, through a detailed description of its morphological, geomechanical and structural features. An integrated multi-disciplinary approach was performed to achieve a clear comprehension of the phenomenon. Field surveys and aero-photo interpretation were carried out in order to clarify the structural, geological and geomorphological setting in which the DSGSD developed. A kinematic conceptual model of the slope deformation was developed through the analysis of morpho-structures, of their significance and relationships with lithological markers and Quaternary deposits. After a geomechanical characterisation of the rock mass involved in the slope deformation, numerical modelling was performed to verify the hypotheses made on kinematics and driving factors of the phenomenon. The sackung affects pre-Permian metapelites, metabasites and marbles belonging to the Upper Austroalpine basement of the Campo Nappe, as well as Late Pleistocene and Holocene glacial and rock glacier deposits. The deformation started after the Late-Wurmian age (15,000–11,000 years B.P.), and continued until few centuries ago, not excluding a present-day low-rate activity. Deformation consists in a large oblique "sagging" along a deep confined sliding surface, associated with gravitational reactivation of pre-existing (late-Alpine and recent) tectonic brittle structures, leading to the formation of N–S and WNW–ESE trending gravitational morpho-structures. The evolution of the WNW–ESE trending system, resulting in asymmetric trenches, led to progressive failure of the lower part of the slope during the last 10,000 years, as testified by large paleo landslide accumulations, and it is still in progress. Numerical modelling indicates post-glacial unloading as the main triggering factor of the slope deformation. The importance of this deep-seated slope deformation is enhanced by the occurrence of the 30 Mm^3 active "Ruinon" landslide in the lower part of the slope. Such landslide is subjected to rapid evolution and threatens the valley floor, establishing an important risk factor connected to human lives and socio-economic activities. © 2001 Elsevier Science B.V. All rights reserved.

Keywords: Deep-seated gravitational deformations; Slope stability; Central alps; Engineering geology; Structural geology; Numerical modelling

1. Introduction

The definition of "deep-seated slope gravitational deformation" (DSGSD) has become more and more important since the 1940s, when the first attempts to understand these phenomena were made (Stini, 1941; Van Bemmelen, 1950). During the last four decades a huge scientific literature grew, dealing with several case studies from a wide variety of geological, morphological and structural settings (Zischinsky, 1966, 1969; Nemcok, 1972; Mahr and Nemcok,

* Corresponding author. Fax: +39-02-70638261.
E-mail address: giovannib.crosta@unimib.it (G. Crosta).

0013-7952/01/$ - see front matter © 2001 Elsevier Science B.V. All rights reserved.
PII: S0013-7952(00)00066-1

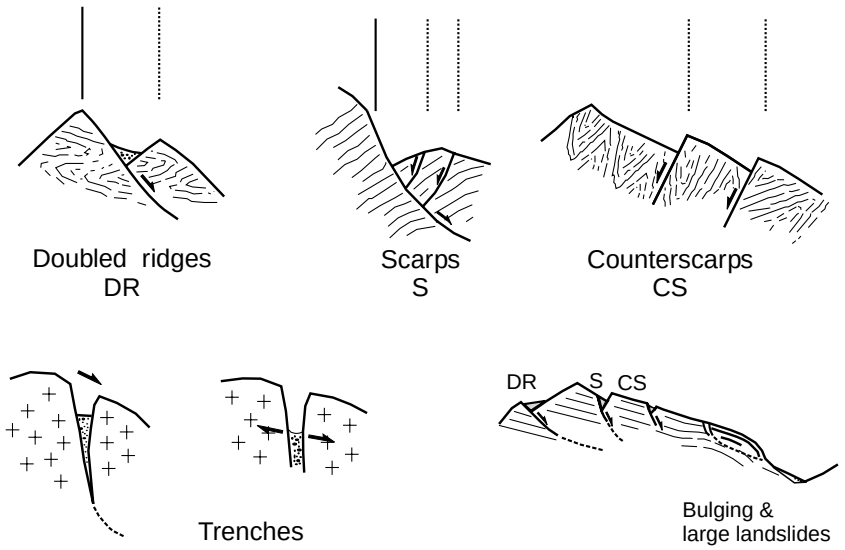

Fig. 1. Morpho-structural features typical of a DSGSD. Two main symbols have been adopted to represent the existing structural elements and to attribute a kinematic significance to them.

1977; Radbruch-Hall, 1978; Bovis, 1982; Savage and Varnes, 1987; Chigira, 1992; Crosta, 1996). Nevertheless, DSGSD are still poorly understood phenomena.

Slope deformations, known as DSGSD, have been defined by authors in different ways, depending on the study approach and on the postulated evolutionary mechanisms. The term "deep-seated deformations" indicates, according to the literature, slope movements occurring on high relief-energy hillslopes, with size comparable to the whole slope, and with displacements relatively small in comparison to the slope itself. These phenomena show evident morpho-structural features (doubled ridges, ridge top depressions, scarps and counterscarps, trenches, open tension cracks, etc. (see Fig. 1; Jahn, 1964; Zischinsky, 1966, 1969; Ter-Stepanian, 1966; Beck, 1968; Patton and Hendron, 1974; Tabor, 1971; Radbruch-Hall et al., 1977; Mahr, 1977; Bovis, 1982) with present-day low rate of displacement, often masked by weathering or erosion. We do not think that the absence of a macroscopically clear sliding surface could be assumed as a diagnostic feature or as a conventional boundary (Sorriso-Valvo, 1995) of a DSGSD in comparison with a landslide. In fact, many landslides described in the literature as "confined" (Hutchinson, 1988; Cruden and Varnes, 1993) do not show a well-defined or complete sliding surface until final collapse. On the other hand, many DSGSD observed (at the surface and at depth) by the authors in the Central Alps are characterised by a basal sliding surface. This surface is sometimes partially coincident to a pre-existing tectonic surface, or it must be postulated to justify their kinematics.

According to our experience, not exclusive diagnostic features of DSGSD are:

- morpho-structures (doubled ridges, scarps, counterscarps, etc.) similar to those observable, at a smaller scale, in cohesive soils landslides;
- size of the phenomenon comparable to the slope;
- present day low rate of displacement (mm/y, in alpine and prealpine areas);
- presence of minor landslides inside the deformed mass and ancient collapses of the lower part of the slope.

Many deep-seated deformations were recognised in the Central-Eastern Alps (Zischinsky, 1966; Forcella, 1984; Forcella and Orombelli, 1984; Crosta and Zanchi, 2000), mainly along deep glacial valleys, in fractured schistose rocks (phyllites, mica-schists, paragneisses).

Different hypotheses were made about the origin of

these phenomena. A link between active faults and the genesis of sackungen was proposed by Forcella and Orombelli (1984) for the gravitational structures occurring in Valfurva (east of Bormio, Italy), partially interpreted as surface expressions of neotectonic faults with the same trend. Gravitational processes connected to post-glacial slope unloading have also been mentioned (Nemcok and Pasek, 1969). Unloading is believed to form fractures parallel to the topography and to reactivate previous recent fractures, as in the case of the Mt. Varadega–Mt. Padrio sackung, located few kilometres south of Bormio, along the divide between the Oglio and Adda basins (Forcella, 1984). In many cases gravity may act at quicker strain rates than neotectonics, masking the presence of active faults moving very slowly. Nevertheless, gravitational reactivation of recent fractures accompanied by formation of large DSGSD in high relief slopes seems to be a common feature in the central sectors of the Alps.

An important DSGSD, never pointed out before, was recognised by the authors in the middle part of Valfurva, 5 km east of Bormio (Rhaetian Alps, Italy). Although some DSGSD phenomena have been recognised in the past along the valley (Mt. Vallecetta, Mt. Sobretta, Corna Rossa and Pasquale Valley; Forcella and Orombelli, 1984), numerous unmapped features have been discovered during this research (see Fig. 2). The analysis of kinematics, causes and triggering factors of the phenomenon is the aim of this work.

An integrated approach is proposed, in order to better support a kinematic interpretation of the phenomenon by means of aerial photo interpretation, geological and geomorphological field surveys and numerical modelling.

2. Geological framework

The metamorphic rocks cropping out in the study area belong to the Upper Austroalpine crystalline basement of the Campo Nappe, which extends between the Engadine Line to the W and the Pejo Line to the E (Fig. 3). The Campo Nappe consists of pre-Permian metamorphics, recording a polyphase tectono-metamorphic evolution during the Varisican and Alpine orogeneses (Froitzheim et al., 1994; Gregnanin and Valle, 1995; Conti, 1997). The studied area is located 5 km south of the Zebrù Line, a steep north-dipping fault separating the Campo Nappe from the overlying Ortler Nappe. Along the studied slope a metapelitic unit crops out ("Bormio Phyllites", Bonsignore et al., 1969), which includes minor transposed and isoclinally folded marbles and metabasites. Phyllites are the dominant lithotype and consist of an aggregate of quartz + chlorite + sericite, with minor amounts of biotite, garnet and ilmenite. Phyllitic paragneisses also occur as thin interbedded layers, as well as slightly schistose quarzite. Lenses of marbles up to 70 m thick crop out in the middle part of the slope (Confinale valley, Baite Cavallaro); these are made of coarse grained saccharoidal calcite or of calc-silicate with calcite + chlorite + white micas. The boundary between marbles and phyllites is often transitional. Lenses of prasinites and chlorite-schists up to 30 m thick occur in the upper part of the slope; they consist of aggregates of chlorite + amphibole + epidote with minor quartz, albite and calcite.

A greenschist facies characterises the whole tectono-metamorphic unit. Relics of amphibolites with porphiroblastic hornblende occur in prasinitic layers, testifying an amphibolite facies metamorphism, almost completely overprinted by alpine greenschist retrocession (Gregnanin and Valle, 1995).

Detailed field survey at 1:5000 scale and mapping of meso-structural elements (Fig. 4) distinguish four main deformational events. D_1 phase produced S_1 foliation, isoclinally folded and transposed (i.e. made parallel to the new axial plane direction) by the next D_2. Relicts of S_1 are preserved in F_2 (F = Fold) centimetre-scale isoclinal fold hinges, marked by thin quartz levels in phyllites and prasinites and by micaceous films in marbles. The D_2 phase originated the main foliation S_{1+2} (i.e. with surfaces derived from both D_1 and D_2 deformational phases), defined by alternated micaceous layers and 1–2 mm thick quartz-rich layers. Schistosity S_{1+2} is discrete, planar in quartz-rich levels, ondulated or anastomosing in phyllosilicatic layers.

The S_{1+2} foliation is crenulated and folded at a different scale by the D_3 phase. F_3 folds are asymmetrical, non-cylindrical and characterised by axial surfaces moderately dipping to N–NE, with sub-horizontal NW–SE striking hinges. Chevron folds (F_3) are recognisable SE of S. Antonio Valfurva (Fig. 4) and indicate a zone characterised by a greater amount of

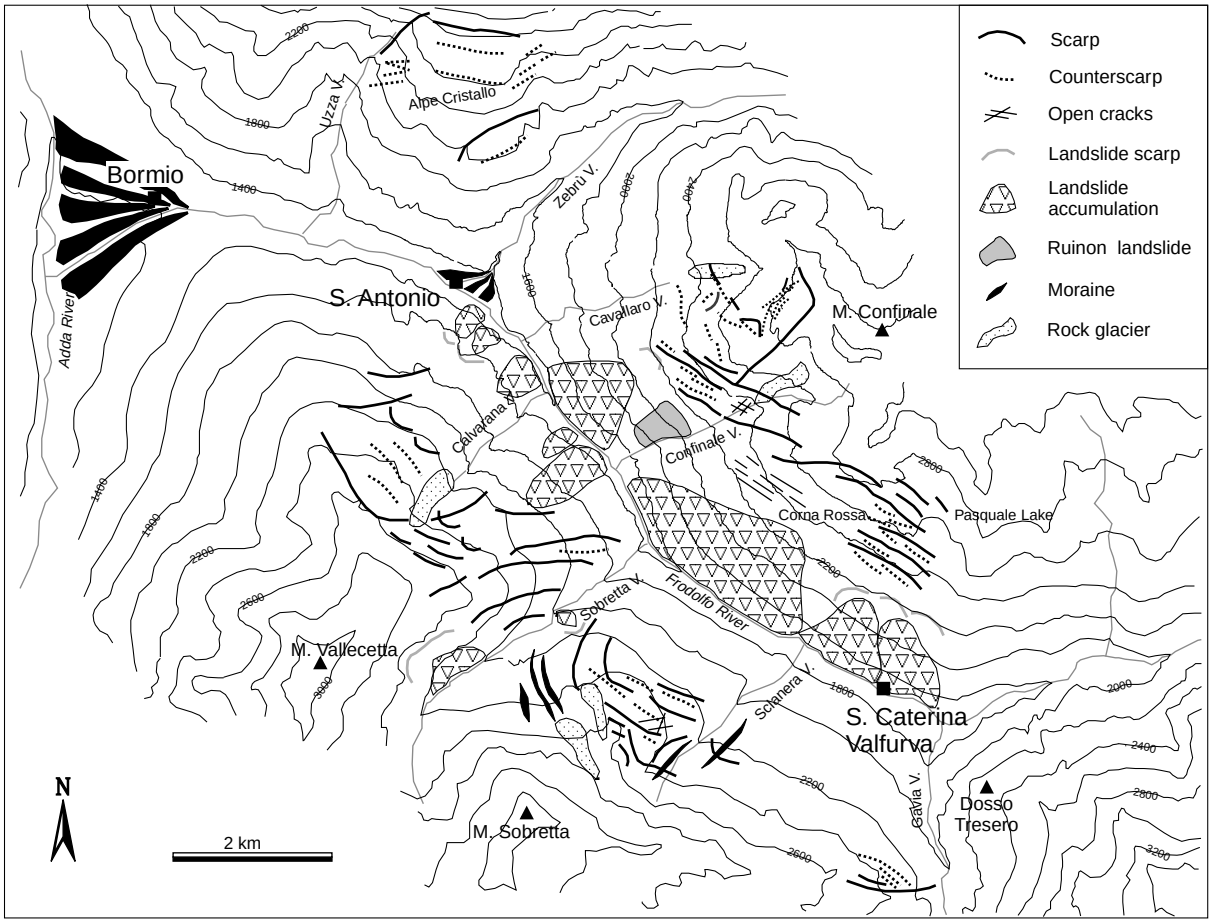

Fig. 2. DSGSD and landslide features along the Valfurva as obtained from aero-photo interpretation. Main trends for the DSGSD features are recognisable together with relationships between them and the periglacial deposits (rock glaciers).

ductile deformation. D_1 and D_2 phases have been referred to Varisican orogenesis, while D_3 has been considered to be Alpine in age (Gregnanin and Valle, 1995). Structures are refolded by a later non-schistogen D_4 phase, consisting in a gentle kilometre-scale folding with subvertical axial surfaces and hinges N55 trending (plunge of 30–35°). F_4 folds (see Fig. 4), show interference patterns (of type 2 according to Ramsay, 1967) with D_3 structures. F_4 folding becomes gentler downslope until it is no more recognisable. This suggests that D_4 structures could be related to progressive deformation on the shear zone of the Zebrù Line (few kilometres north of study area, Fig. 3), characterised by "top-to-WNW" overthrusting during Cretaceous orogeny of Austroalpine units (Trupchun phase according to Conti, 1997).

3. Morpho-structural analysis

3.1. Geomorphological settings

Knowledge of geomorphological features is a fundamental step for the understanding of the history of a slope affected by DSGSD. Analysis of aerial photos (T.E.M.-Regione Lombardia, 1981, 1:20,000 scale) and field surveys carried out at 1:5000 scale revealed the presence of several different types of

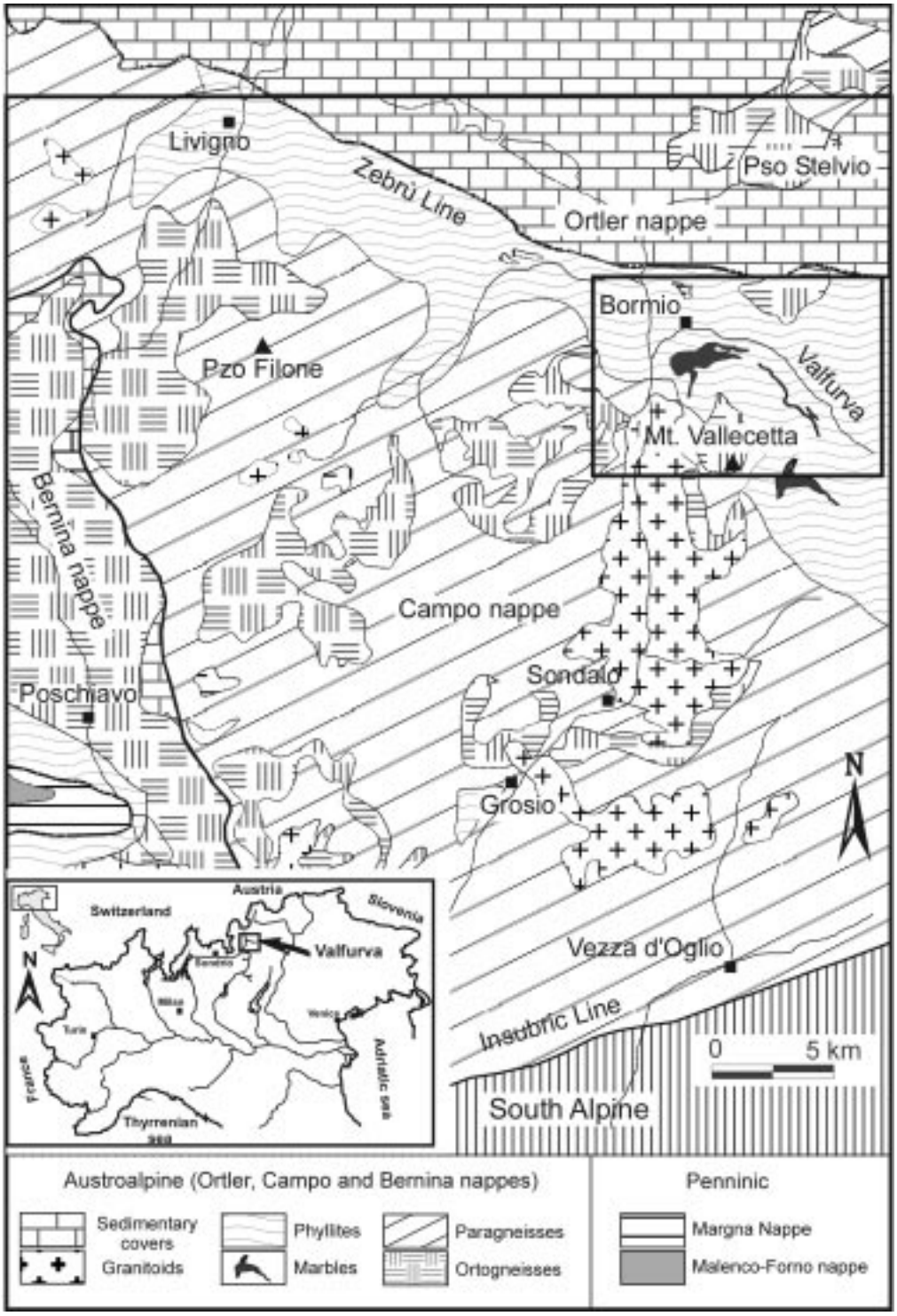

Fig. 3. Location map of the study area and geological sketch of the Upper Valtellina with the main structural features.

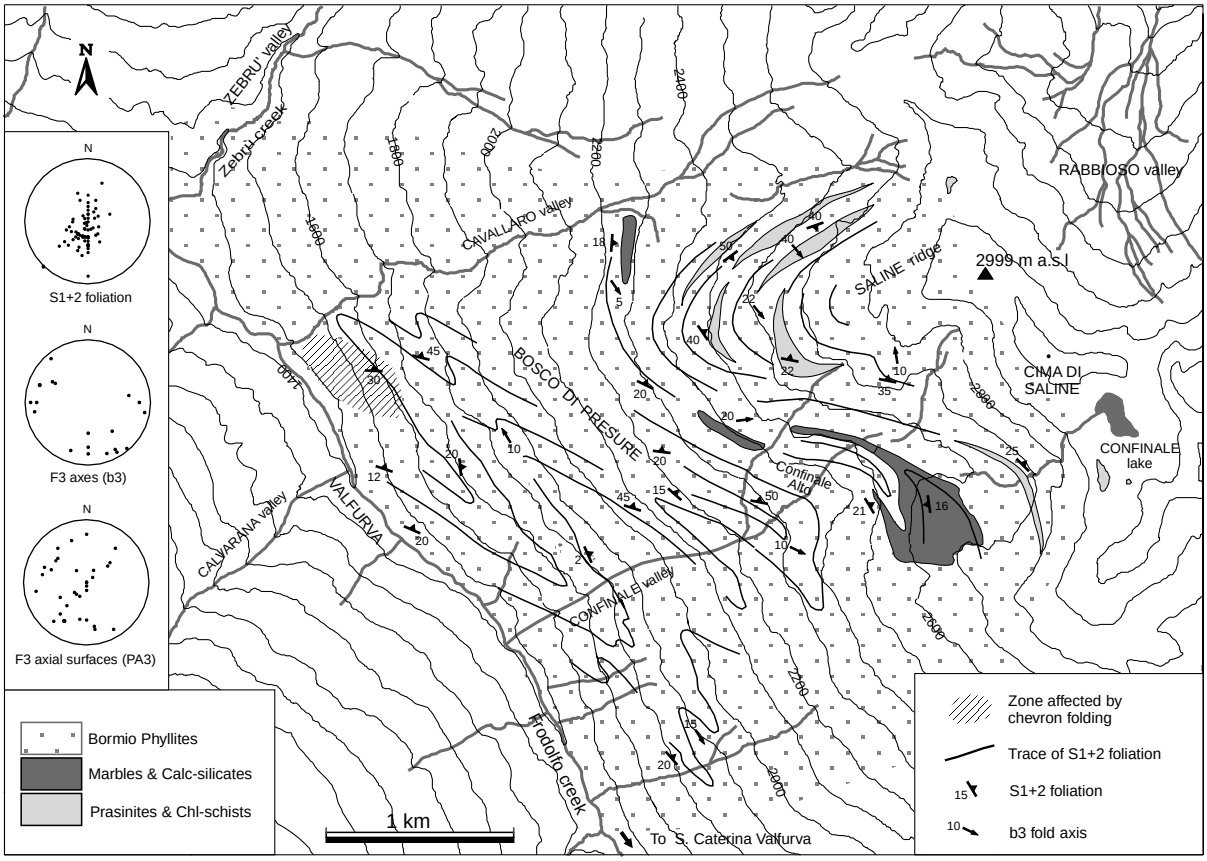

Fig. 4. Interpretative geo-structural map of the study area, reporting meso-structural features and the related stereoplots (Schmidt's lower hemisphere projection).

landform, suggesting a complex evolution of the area during Late Pleistocene and Holocene.

The examined slope is bounded by the Cavallaro and the Confinale valleys (Figs. 2, 4–6). These are right-hand flank tributaries of the Valfurva, a WNW–ESE trending glacial valley deeply cut by the Frodolfo River. The Confinale slope has high relief energy, ranging in elevation between 1350 and 2999 m a.s.l., with a maximum elevation difference of 1649 m.

In order to represent the general morphological and deformational pattern, a digital elevation model (DEM) was obtained through different CAD/GIS packages (AutoCad, ILWIS). A geo-referenced contour map in a vector format (obtained from the "Carta Tecnica Regionale della Lombardia", scale 1:10,000) has been converted into a raster grid with a pixel size of $10 \times 10\ m^2$, and then interpolated. The DEM obtained in such a way has been used to produce a shaded relief map (Fig. 5).

Morphometric analyses of the so obtained DEM outlined a lower sector with a steep (slope angle ranging from 30 to 35°), slightly convex profile, and a strongly convex upper part, with a mean inclination of 20°.

Superficial deposits cover most of the area (see Fig. 6). They are mainly Late Pleistocene and Holocene glacial deposits (Catasta and Smiraglia, 1978), rock glacier deposits (Holocene; see Fig. 8), talus, landslide, outwash and alluvial deposits.

Many glacial erosional forms are recognisable, such as lateral perched valleys (Zebrù, Cavallaro

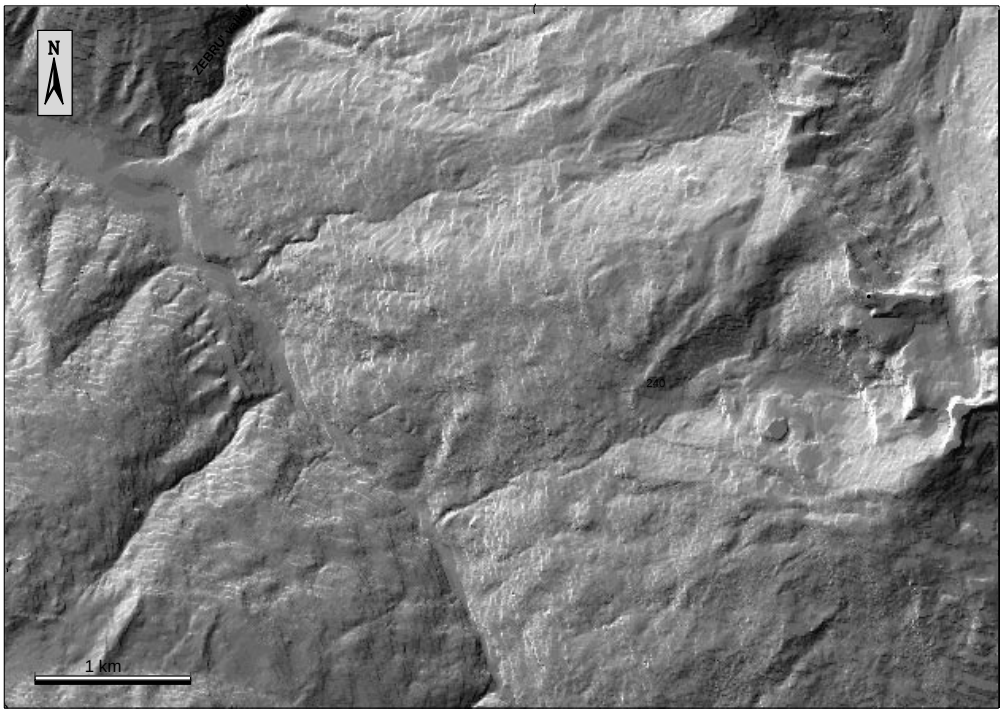

Fig. 5. Shaded relief map based on the DEM performed with a 10×10 m^2 pixel raster grid, from the 1:10,000 scale topographic map (area as in Figs. 4, 6, 7 and 9).

and Confinale valleys; Fig. 7), cirques (upper Confinale valley), striated surfaces and roches moutonèe. Accumulation forms are also present, such as terraces and moraines.

Periglacial forms as large Holocene rock glaciers are recognisable along the Cavallaro and Confinale valleys, between 2300 and 2675 m a.s.l. (Fig. 7). One of them (upper Confinale valley) is considered "uncertainly active" (CNR-Gruppo Nazionale Geografia Fisica e Geomorfologia, 1997). Rock glaciers show typical "convex tongue" shapes with steep fronts and are cut by transversal scarps related to gravitational deformation of the slope (Figs. 2, 9 and 10).

Some relict rockslide accumulations, covered by vegetation, have been detected on the slope, the most important of which is located just downslope of "Bosco di Presure" (Fig. 9). This is a composite body of post-Wurmian age with a structurally controlled detachment scar. Spreading of the accumulation on the valley floor created a natural dam, as we can infer from the knee point and the narrowing of the valley (Figs. 5 and 9). Southeast of this landform, a 30 Mm^3 active landslide, known as "Ruinon landslide" is recognisable (see Figs. 5 and 10). This phenomenon has been studied by the authors (Crosta et al., 1999) through field surveyings, borehole and superficial monitoring data. As a consequence, the present-day kinematic evolution and the associated hazard for this sector of the DSGSD toe have been inferred.

3.2. Tectonic lineaments

More than 300 fractures and faults were measured in the field in six sites (see Fig. 11), and several lineaments were identified through the observation of aerial photos. Four main sets of structures were recognised:

- WNW–ESE striking set of subvertical or SSW steeply dipping fractures, including master joints and faults;
- N–S oriented subvertical fractures;
- NE–SW striking joints and normal faults, steeply dipping to NW or SE;

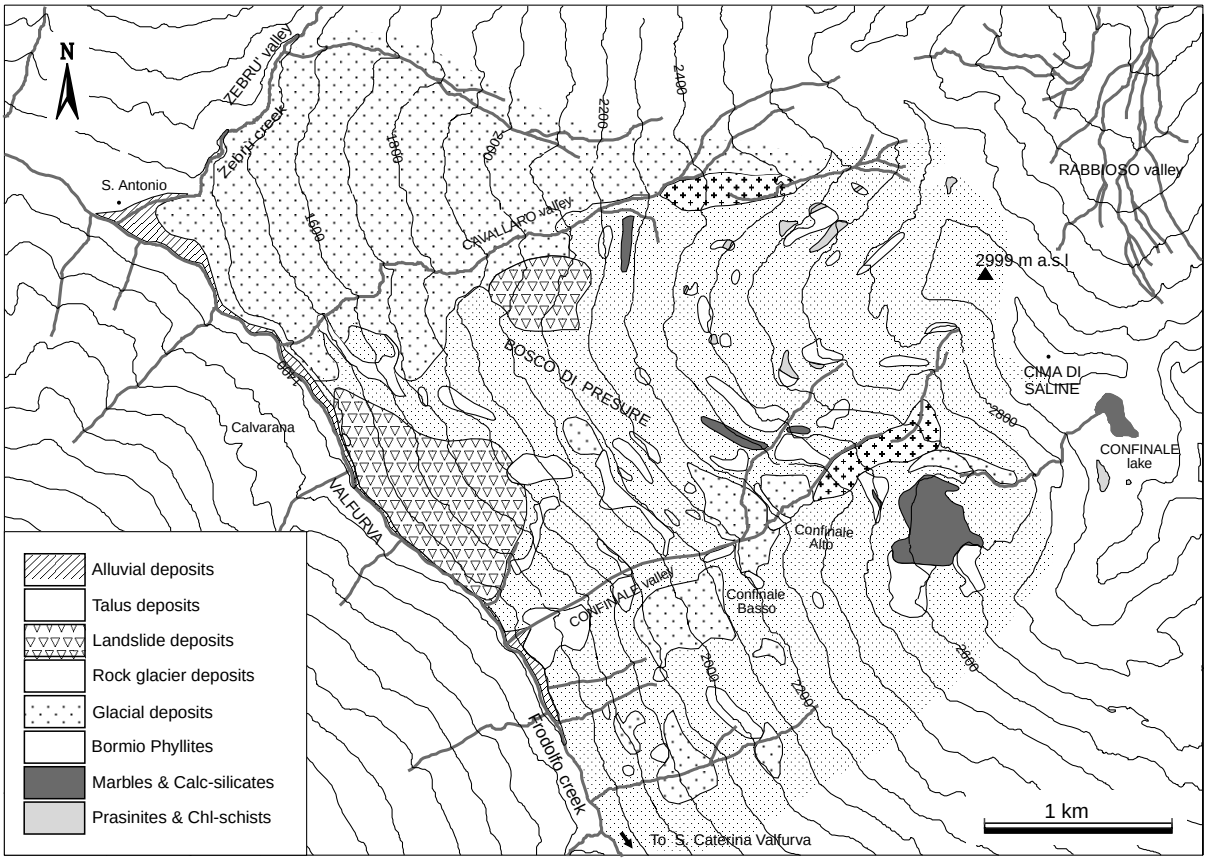

Fig. 6. Lithological map of the study area, showing the distribution of lithotypes and superficial deposits.

- E–W trending subordinate set of subvertical fractures.

WNW–ESE and N–S trending fracture systems are the most frequent in the area. This could suggest a recent activation of these structures, which seem to interrupt the continuity of the NE–SW trending set. This observation is in agreement with Forcella et al. (1982) and with the orientation of the main DSGSD features reported in Fig. 2. These fractures strongly influence the trend of the valleys, such as the WNW–ESE trending Valfurva. The same trend is followed by the upper part of the Zebrù Valley which is NE–SW oriented in its lower part. Trend analysis of photo-interpreted lineaments (Fig. 6), performed by means of a GIS software (ILWIS) clearly enhances the influence of WNW–ESE and NE–SW trending brittle structures on the drainage pattern. Regional WNW–ESE and local N–S trending fractures strongly control the development of the DSGSD and landslides (Fig. 10).

3.3. Gravitational morpho-structures

The term "morpho-structure" is used here to describe the morphological expression of a deformational structure of tectonic or gravitative origin or by their interaction. The comprehension of the kinematic meaning of these superficial evidences has a primary role in the study of a deep-seated gravitational deformation.

Morpho-structures have been described and mapped in the past prevalently with a morphological approach. Terms as "scarp", "up-hill facing scarp" or "antislope scarps" (Radbruch-Hall et al., 1977; Bovis, 1982) have been used to point out an upward or downward facing break in the slope profile with different

Fig. 7. View of the Saline Ridge area, in the foreground, bounded by the Cavallaro valley (on the left) and the Confinale valley (on the right). The upper sector of the DSGSD (between 2300 and 2999 m a.s.l.) with the main scarp (triangular facet at the centre of the photo), the Confinale cirque and the rock glacier is shown.

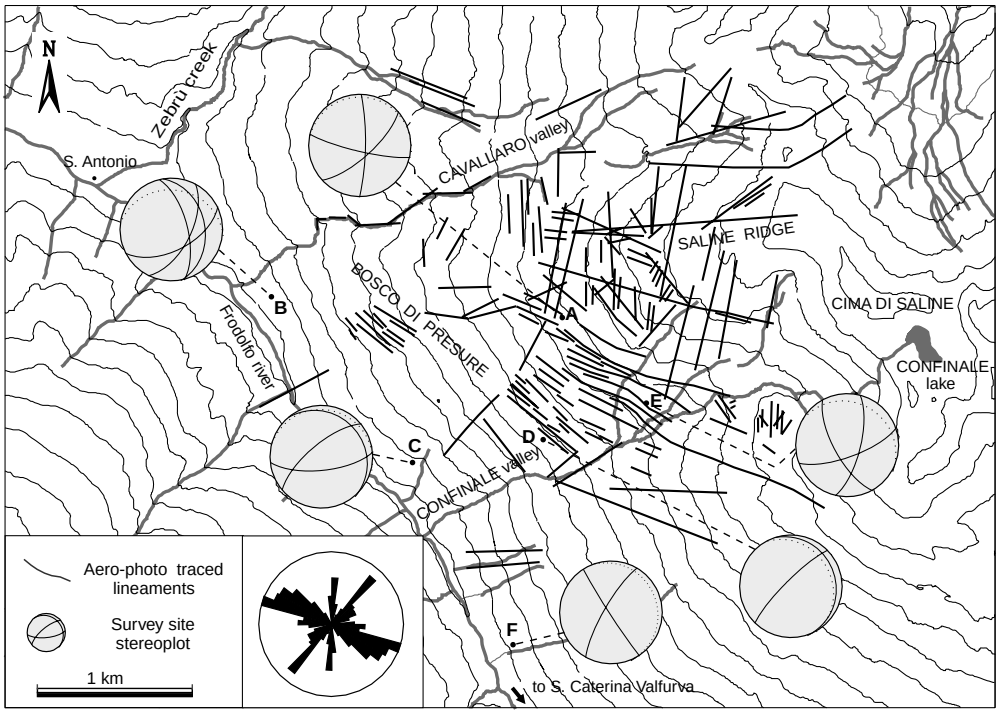

Fig. 8. Map of the lineaments traced by photo-interpretation (brittle structures and DSGSD features) and Rose diagram (relative frequency of lineament trend for 7.5° classes). Stereoplots (Schmidt's lower hemisphere) with the main joint sets and foliation for each of the six structural and geomechanical survey sites are reported.

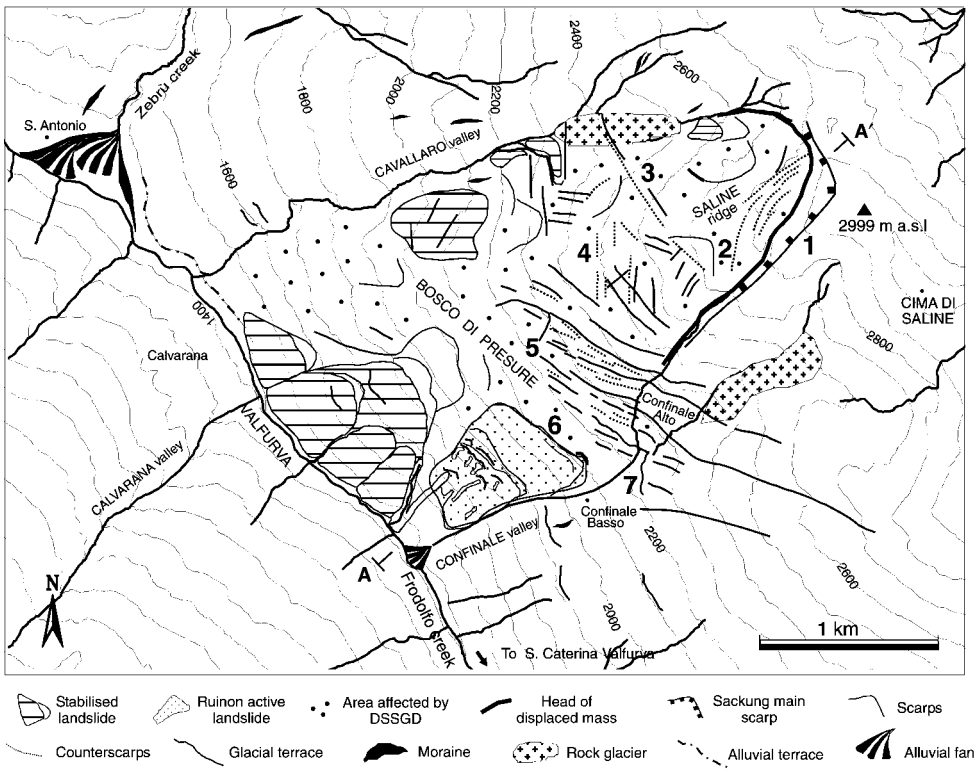

Fig. 9. Geomorphological and morpho-structural map of the study area. Numbers denote features referred to in the text and in successive Fig. 10.

origins. Hutchinson (1988) distinguished three main types of feature: DD (normal down slope down movement facing scarps), UD (up slope down movement facing counterscarp), UU (up slope up movement facing counterscarp), but again no complete information is given about the kinematics. In fact, Hutchinson (1988) states that in this classification "movement is used in the sense of the overall, eventual slide movement, not a local movement associated with scarp formation". All these kinds of approach caused some misunderstanding in the kinematic interpretation of the DSGSD structures. The term "up-hill facing scarp", for example, could either indicate a morpho-structure which bounds downslope the head of a tilted mass, displaced along a downslope dipping subcircular surface (case DR in Fig. 1), or an obsequent (antithetical) collapse surface (cases S and CS in Fig. 1). In this work an effort has been done to give a kinematically consistent nomenclature and cartographic symbology in order to minimise ambiguities. According to this approach, the following terms have been adopted (see Figs. 9 and 10):

- *Scarp.* Morphological expression of a downhill dipping collapse or main failure surface with a downslope movement (continuous lines in Figs. 1, 2 and 9);
- *Counterscarp.* Surface evidence of an upward dipping surface, standing alone or antithetically associated to a major scarp with an upslope movement (dashed lines in Figs. 1, 2 and 9)
- *Trench.* Linear and deeply cut form, expression of extensional opening of a vertical or downward dipping surface.

In the study area, detailed analysis of the Saline Ridge (Figs. 9 and 10) pointed out a huge downward displacement of the upper part of the slope (Figs. 7 and 12), causing the splitting of Saline Ridge and of the crest-line between Valfurva and Zebrù valley. At

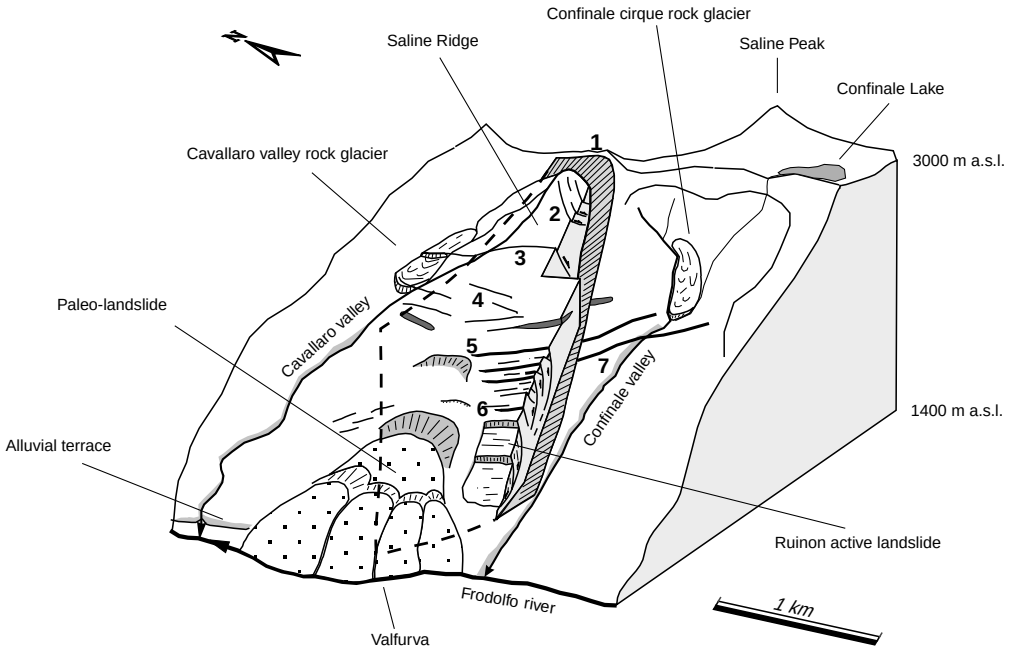

Fig. 10. 3D model of the sackung, reporting the main features referred to in the text and in Fig. 9. The shaded sector and the dashed line represent the 3D geometry of the main failure surface postulated by connecting both superficial (main and lateral scarps, see Figs. 5, 8 and 9) and deep elements.

the top of the slope, a NNE–SSW trending scarp (triangular facet, Fig. 7), dipping downward at 30° (no. 1 in Figs. 9 and 10) and covered by blocky debris (Fig. 12), is recognisable. Antithetical listric collapse surfaces are associated to the main scarp (no. 2 in Figs. 9 and 10). The maximum recorded displacement along the main collapse surface exceeds 140 m. The superficial evidences of the main scarp can be followed

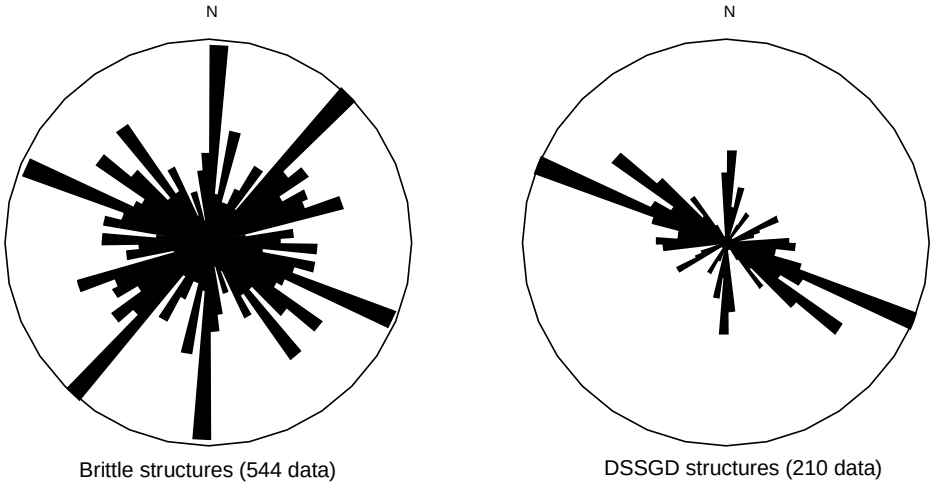

Fig. 11. Rose diagrams (5° intervals) comparing frequency distributions of brittle tectonic (structural surveys and photo interpretation) and DSGSD structures (see Fig. 6).

Fig. 12. Close view of the main scarp of the sackung (see triangular facet in Fig. 8 and no. 1 in Fig. 10) at the upper end of the Saline Ridge.

downslope along a NE–SW trending blind valley (Figs. 5, 8 and 9) which disappears below 2200 m.a.s.l.

A NW–SE striking lineament (no. 3 in Figs. 9 and 10) was also traced in the middle part of Saline Ridge. It consists of a system of subvertical or steeply upslope dipping planes, which seems to bound an "active wedge" at the top of the slope. The lineament cuts the metamorphic basement as well as the rock glacier of the Cavallaro valley (Fig. 9).

Two swarms of morpho-structures are recognisable between 2100 and 2650 m a.s.l. They strike N–S and WNW–ESE and fit the two most important clusters of joints, recognised during the field survey (Fig. 11).

N–S trending structures (no. 4 in Figs. 9 and 10) mainly consist of rectilinear counterscarps up to 300 m long. They affect the substratum and the rock glacier deposits and are expressions of upward steeply dipping shear surfaces, with a maximum upslope directed throw of 3–4 m.

The WNW–ESE striking swarm (no. 5 in Figs. 6 and 12) is mostly present below 2350 m.a.s.l. and consists of 55–70° dipping scarps, up to 1.5 km in length, with associated minor antithetical counterscarps (Fig. 13). Systems of scarps and counterscarps form "half graben-like" asymmetric features upto 20–30 m wide (Figs. 10 and 14). These are filled with blocky debris and show an average displacement of 20 m. Both the bedrock and the superficial deposits (slope, glacial and periglacial) are interested by these structures and open tension cracks (up to 4 m opened). Near Confinale Alto a glacial terrace is lowered down with a throw of 30 m (no. 7 in Figs. 9 and 10).

Moving downslope, structures progressively change from half-grabens to rectilinear or downward convex trenches and tension cracks (no. 6 in Figs. 9 and 10). These features are up to 5 m wide and show strong evidences of activity (fresh collapse surfaces, toppled and crashed trees, stretched roots, etc.) until 2100 m.a.s.l., where the crown of the "Ruinon" active rockslide occurs.

No important morpho-structures can be recognised on the lower part of the slope, but large

Fig. 13. Scarps and conterscarps upstream of the Bosco di Presure (about 2250 m a.s.l., see no. 5 in Fig. 9).

paleo- landslides occur. These are evidences of ancient instabilities and collapses of the lower part of the slope. Paleo-landslide accumulations break the continuity of an alluvial terrace in a huge till deposit SE of Sant'Antonio (Figs. 6, 9 and 10). This suggests a post-Wurmian age for the collapse. Again, the geometry of the landslide scarps is controlled by WNW–ESE directed fractures, supporting the idea of a strong structural control on the slope gravitational deformation.

3.4. Kinematic interpretation, age and state of activity

The recognised morpho-structural setting suggests a kinematic interpretation of the phenomenon. The slope is affected by a sackung-type gravitational deformation, developed along a deep-seated, maybe confined, sliding surface (Figs. 5, 9, 10 and 14). Such WNW dipping surface is oblique to the dip direction of the slope and it is slightly listric. The mass movement is strongly asymmetric, probably because of the structural control of pre-existing brittle structures on the geometry of the main sliding surface. The Saline Ridge area has been displaced downslope with a WNW component of motion. Morphological and lithological markers (no. 1 in Fig. 10) suggest a downward displacement of 120–140 m in the upper part of the slope.

According to our interpretation, the displacement of the upper part of the slope was accompanied, in the middle part, by reactivation of WNW–ESE trending fractures. Starting from pre-existing discontinuities, listric faults (see cross section in Fig. 14) associated to antithetical minor dip slip surfaces developed, forming asymmetric trenches. Extension along these structures increased the amount of deformation in the lower part of the slope, taking to the development of rotational rockslides, already occurred or still active, as the "Ruinon" landslide suggests.

The age of the gravitational deformation can be obtained from the relationships between morpho-structural features and Quaternary landforms and

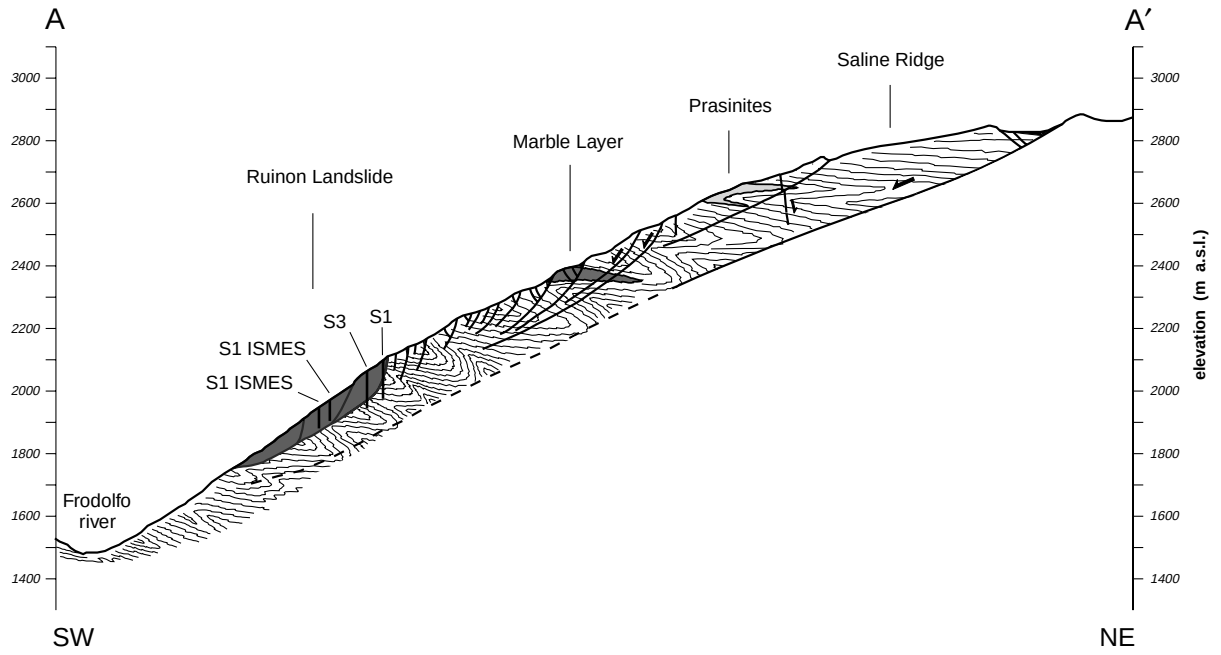

Fig. 14. Geological and morpho-structural cross section through a SW–NE trace (see Fig. 9).

deposits. Many morpho-structures cut glacial deposits and associated landforms (terraces, edges of Confinale valley cirque, Figs. 9 and 10), referred by authors (Smiraglia, 1981; Pelfini, 1987) to the Late-Wurmian age (15,000–11,000 years b.p.) and, at higher elevations, to Holocene. DSGSD are then post-Wurmian in age, probably younger than 10,000 years.

Rock glaciers occurring in the Cavallaro and Confinale valleys are also cut by DSGSD structures. Calderoni et al. (1993) performed ^{14}C datings on rock glaciers near Foscagno Pass, few kilometres from the study area, obtaining minimum ages ranging from 5000 ± 70 to 770 ± 60 years. The proximity and morphoclimatic similarities between the two areas suggest that these ages can be assumed as valid also for the rock glaciers in the study area. According to these data, the sackung should have been active during the last 5000 years, not excluding any previous activity.

As regards to the present state of activity of the sackung, the lack of monitoring of the upper part of the slope (Saline Ridge area) prevents the assessment of activity. We can only consider morphological evidences of activity, the degree of vegetation cover-age and the relationships with superficial deposits. On these bases, the Saline Ridge area appears to be inactive, although low-rate displacements along structural features, that can be masked by weathering and erosion, cannot be excluded. Evidences of activity increase almost continuously downslope between 2300 and 2100 m.a.s.l., in response to the rapid evolution of the "Ruinon" landslide (Fig. 10). The adjoining paleo-landslide body does not show, instead, significant evidences of activity.

4. Geomechanical characterisation

The evaluation and collection of geomechanical data in large-scale problems is always difficult because of a number of problems, involving sampling, representativity and field-scale extrapolation, especially when dealing with weak rock masses as the Bormio Phyllites. The task is even more difficult in a DSGSD problem, because of their geological and structural complexity. Taking into account a great range of uncertainty on the results, geomechanical characterisation of the rock mass was performed in

Table 1
Summary of the geomechanical observations performed in the field. The location of the six survey sites is reported in Fig. 6

Site	Lithology	RMR (Bieniawski, 1989)	Number of joint sets	JRC (Barton, 1976)	JCS (MPa) (Barton, 1976)	Weathering (ISRM, 1978)
A	Marble	47	4	10–13	11.8–14.7	W2
B	Phyllite	45	5	13–17	15.7–25.5	W2
C	Phyllite	60	4	10–18	16.2–38.7	W2
D	Phyllite	55	3	9–14	11.8–28.4	W2
E	Phyllite	47	4	6–13	27.9–42.1	W1 to W2
F	Phyllite	70	3	12–18	9.8–26.9	W2

order to obtain reasonable values for the mechanical parameters required by the numerical modelling. Data were acquired through few available literature data (Canetta et al., 1992), field surveys and measures, empirical correlations (Barton and Choubey, 1977; Hoek and Brown, 1980) and some laboratory testing.

Six geomechanical surveys (locations and stereoplots in Fig. 8) were carried out, in order to collect information about rock material, features of discontinuities, alteration and water conditions. A statistically representative number of measures of fracture orientation was collected and analysed through stereographic projections (Schimdt's Net). Joint roughness coefficient (JRC; Barton, 1976) and joint compressive strength (JCS) field assessment was performed on a large number of discontinuities through simple equipment (pocket shape tracer and Schmidt hammer). Geomechanical field description is summarised in Table 1. A number of rock samples taken from drill cores (S3 borehole, Fig. 14) was also tested in laboratory through uniaxial compression (20 samples) and "Brazilian" indirect tension tests (20 samples). This allowed to obtain the average values of uniaxial compressive strength (73 MPa, $\perp$ to the foliation plane) and uniaxial tension strength (12 MPa, $\parallel$ to the foliation plane) of intact rock.

Table 2
Geomechanical properties of the rock mass, obtained from field measures, empirical correlations and laboratory testing as used in the numerical modelling

Property	Units	Average value
Mass density	kg/m^3	2750
RMR rating (Bieniawski, 1989)		54
Q index (Barton, 1976)		4.85
E (rock mass Young modulus)	GPa	11
K (bulk modulus)	GPa	10
G (rock mass shear modulus)	GPa	5
mi (Hoek and Brown, 1980)		10
mb (Hoek and Brown, 1980)		0.37
s (Hoek and Brown, 1980)		0.0005
t (rock mass tensile strength)	MPa	0.1
c (rock mass cohesion)	MPa	0.2
ϕ (rock mass friction angle)	°	32

Data were elaborated, reduced and used to rate the rock mass by means of RMR (Bieniawski, 1989) and Q-system (Barton, 1976) geomechanics classifications. Average values of RMR rate and Q index made it possible to obtain, through empirical correlations (Hoek and Brown, 1980; Bieniawski, 1989), the most important geomechanical properties of the rock mass (summarised in Table 2).

Five boreholes up to 116 m deep were performed by the Geological Survey of Regione Lombardia in the Ruinon landslide area, in order to appraise subsurface data for the landslide study. The data, obtained during a study by the authors (Crosta et al., 1999) were examined and the stratigraphy of a core from a borehole located at 2000 m a.s.l. on the left side of the "Ruinon" landslide, was described. This allowed to distinguish weak and cataclastic zones up to 2 m thick, characterised by RQD = 0 and filled with sandy silt, at depth of over 90 m. At the present state of knowledge we cannot infer the correct origin of these shear zones. In fact they could be related to either a sackung activity or a former brittle tectonics. The occurrence of such deep weak zones supports the hypotheses made on the kinematic evolution of morpho-structures in the lower part of the slope, according to the field analysis.

5. Numerical modelling

A numerical model concerning the slope evolution across post-Wurmian times was performed with a

A) Initial conditions

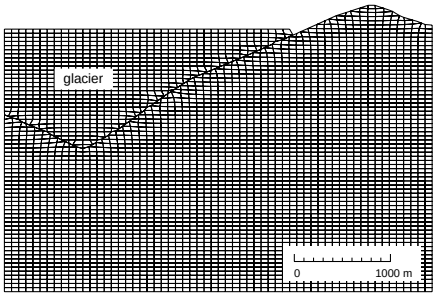

B) After 46,000 steps

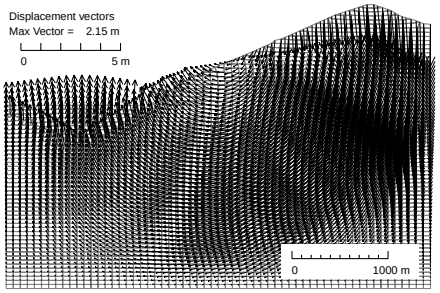

C) Final condition (66,000 steps)

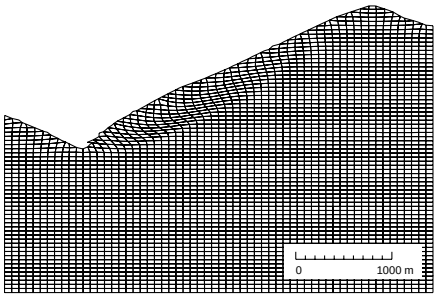

D) Orientation of anisotropy (66,000 steps)

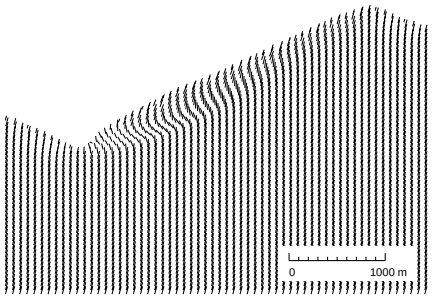

E) Total displacements (66,000 steps)

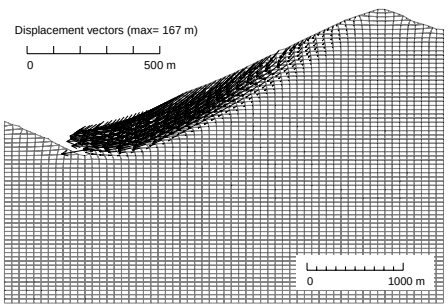

F) Plastic state (66,000 steps)

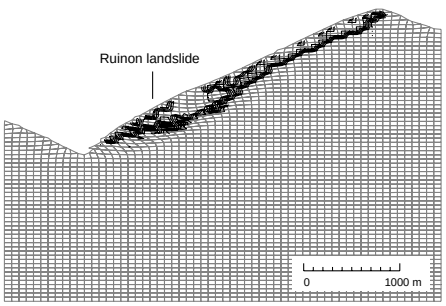

G) x - velocity contours (66,000 steps)

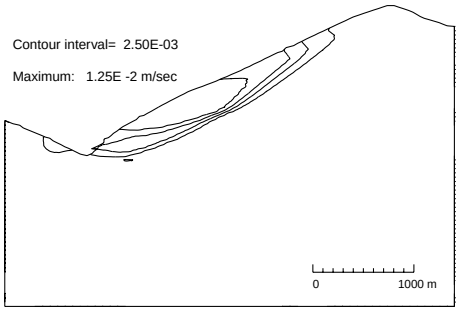

H) y - velocity contours (66,000 steps)

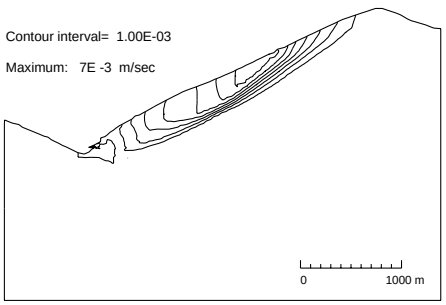

two-dimensional (2D) geomechanical simulation code (FLAC v 3.40, ITASCA, 1998) based on the explicit finite difference method. Simulations were performed in order to test the mechanical consistency of the kinematic hypotheses made about the evolution of the slope, and to make numerically supported considerations about the driving and triggering factors of the sackung. In order to obtain more realistic results, as many as possible geological, geomorphological and geomechanical constraints were included (anisotropy, fracturing, geomorphic history, etc.).

The NE–SW directed cross section A–A′ (Fig. 9) was chosen for the model because of the larger amount of available data. The slope profile was restored to a reasonable "glacial age" condition, taken as an initial geometry for the simulation. A 60×75 finite difference grid was generated, fitting the cross-section profile and extended up to the sea level, in order to minimise the "boundary effects". The grid was constrained by displacement-type boundary conditions (fixed bottom and no lateral horizontal displacements allowed). Different types of constitutive relationship have been adopted in different models (elasto-plastic, strain softening, Burger's viscoplastic). After a number of test model runs, a "ubiquitous joints" constitutive model (ITASCA, 1998) was chosen, assuming an elasto plastic material with a transversal anisotropy dipping at 75° downslope with respect to the horizontal. This anisotropy represents the pervasive subvertical WNW–ESE trending joints, in a Mohr–Coulomb failure context. Geomechanical properties of rock mass (see Table 2), obtained from field survey, empirical correlations, laboratory testing and literature data, were assigned to the zones representing the slope. The grid region representing the Valfurva, between valley floor (1400 m a.s.l.) and 2750 m.a.s.l., was imposed to represent a glacier (Fig. 15A). Mechanical properties of ice were assumed from literature data. The maximum elevation reached by the glacier (2750 m) was supposed on the basis of geomorphological field data. Gravity acceleration and in situ stress with a horizontal N–S directed σ_1 (Westaway, 1992) were applied. Groundwater conditions have been simulated by imposing boundary conditions with different hydraulic head values during the different steps of the simulation. The assumption was that of a changing parabolic groundwater table profile intersecting the slope profile at the elevation reached by the glacier surface at the same "time interval". The slope evolution was simulated through a "sequential modelling" approach (with computational time not directly related to actual time), consisting of a progressive change of conditions, properties and applied forces, reproducing physical and mechanical variations of the real system. The model was first run to reach equilibrium with respect to the initial conditions, in order to minimise inertial effects. Then glacier removal was simulated by progressive elimination of thin ice layers, to reproduce the post-Wurmian glacial debutressing of the valley. During the glacier removal phase of the simulation (Fig. 15B) the model has shown a tendency to an elastic rebound of the slope and of the valley floor, without significant failures. After the complete removal of the glacier a new equilibrium was reached. A huge increment of deformation occurred (Fig. 15C–E), with a lowering of the upper part of the slope (above 2300 m a.s.l.) and a bulging of the lower sector (Fig. 15C and D). Failure occurred at various locations in the model, as suggested by the monitoring of grid displacements, whose entity, up to 170 m, is similar to that recorded by morpho-structures. The pattern of displacements and plasticity indicators (Fig. 15F) also point out the presence in the model of a 200–300 m deep basal slip surface with a similar geometry with respect to that postulated by the proposed kinematic mechanism (Fig. 14). Significant sliding along downward dipping joints has also been detected, providing evidence of mechanical consistence for the gravitational reactivation of pre-existing fractures. Moreover, it is important to note that some test models, run without introducing the joints, did not show the huge displacements observed in the field. This suggests

Fig. 15. Results of the numerical elasto-plastic model performed by finite-difference method (FLAC v 3.40, ITASCA, 1998): (A) initial conditions; (B) total displacement vectors at the end of the glacier removal; (C) final geometry of the finite difference grid; (D) final orientation of the transversal anisotropy (initial dip: 75°; ubiquitous joint model); (E) total displacements at the end of the simulation; (F) plastic state: lines connect zones that satisfy the yield criterion, delineating failure surfaces on which plastic flow occurs; (G) instantaneous x-velocity contours; and (H) instantaneous y-velocity contours at the end of the simulation.

that structural control could be a necessary condition for the development of the phenomenon.

In addition, two more important observations can be made about the results. First of all, the outcropping of the main shear zone (basal failure surface) occurs just uphill of the valley talweg as suggested in Fig. 10 from field observations. Second, a superficial failure (Fig. 15F) is evidenced in correspondence of the toe bulging in the same position where the active Ruinon landslide (Fig. 10) and the old landslides can be found.

The model shows a reasonably good similarity with the actual slope, showing mechanisms and entity of deformation that are very close to those observed in the field. Some differences between the model and the slope were detected as far as concerns the spatial distribution of displacements. In fact, the model does not show the huge double crested ridge at the top of the slope, well observable in Saline Ridge area, and is characterised by excessive displacement in the lower part. This could be related both to the absence in the model of a discrete feature (master joint or fault) controlling the displacements and the strong asymmetrical geometry of the phenomenon. This three-dimensional (3D) effect cannot be taken in account by a 2D (plane strain) model. Nevertheless, plastic state and tensile failure are observed in the model close to the main ridge.

6. Discussion and conclusions

Field investigations allowed to recognise an important deep-seated slope gravitational deformation affecting the whole slope between the Cavallaro and the Confinale valleys, in the Valfurva, a few kilometres north of Bormio. According to field observations and available datings of glacial deposits, the sackung began to move after the glacial debutressing, at the end of the Wurmian glaciation, continued to recent times and it is possibly still active at low to very low rates of displacement. The slope deformation consists of a large oblique (i.e. transversal to the slope direction) "sagging" along a structurally controlled deep confined sliding surface and associated with gravitational reactivation of recent pre-existing tectonic fractures. The DSGSD led to the formation of N–S and WNW–ESE trending trenches, scarps and counterscarps. The evolution of the WNW–ESE system, forming asymmetric trenches, led to the progressive bulging and failure of the lower part of the slope during the last 10,000 years and is still in progress in the area of the active "Ruinon" landslide. The kinematics of the Ruinon landslide appear to be strictly linked to that of the whole slope, as suggested by the continuous downslope increase of activity along the WNW–ESE trending morpho-structures, located above the landslide crown. From a geological and structural point of view, three main factors are retained as relevant for the understanding and modelling of the slope evolution. First of all, the presence of a sector characterised by chevron folds at the slope toe which could act as a weakness point for the initiation and propagation of a failure surface. Second, the sub-horizontal trend of the foliation could allow the exit of the failure surface in coincidence or uphill of the valley talweg. Third, the brittle tectonic structures control both the DSGSD evidenced along the Valfurva (Fig. 2) and the one examined in this study. In fact, these pervasive subvertical discontinuities are the most diffused and important features.

Numerical modelling suggests an anisotropic elasto-plastic behaviour of the rock mass, whereas a "rock creep" mechanism (numerically tested using a Burgers non-linear model) seems to be not suitable to explain the studied phenomenon. The triggering cause of the phenomenon must be related, according to the numerical simulation, to the removal of the glacial confinement in the late Wurmian age. This caused a significant unloading of the slope, followed by formation of failure surfaces and reactivation of pre-existing fractures in response to the extension of the Saline Ridge area. Also, the increased groundwater flow due to the ice melting probably played a major role increasing the amount of pore pressures in shear zones and cataclastic bands. Furthermore, the evolution of the sackung was controlled by driving factors, such as structural features (metamorphic foliations and recent fractures), topography and relief energy and possibly in situ active stresses. This last point is suggested by the earthquakes occurred near Bormio on 29 and 31 December 1999 (maximum seismic magnitude $M_L = 4.9$).

Neotectonic activity has been recognised in Central Alps by means of photo interpretation (Forcella et al.,

1982), seismological data (Slejko et al., 1989) and by mesoscopic analyses and in situ stress determinations (Canetta et al., 1992; Zanchi et al., 1995). Some authors (Forcella and Orombelli, 1984) invoked active tectonics as the triggering cause leading to the formation of morphostructures in Valfurva. Nevertheless, although brittle structures have been recognised to have a fundamental control on the geometry of the sackung, the proposed unloading mechanism gives a better account for field evidences.

The structural control of pre-existing (Alpine and recent) brittle structures revealed to be the most important driving factor of the evolution of this DSGSD and other examined by the authors (Crosta and Zanchi, 2000). In fact, major discontinuities increase the number of degrees-of-freedom in the rock mass kinematics, the effects of alteration and the importance of groundwater flow, allowing large-scale displacements. At the same time, as mentioned above, they constrain the geometry of the deformation, the pattern of morpho-structures and the kinematic evolution of the slope.

The study of DSGSD, in spite of the abundant literature, can yet be considered at the beginning and needs new theoretical developments. In fact, the comprehension of kinematics and causes of phenomena requires complete and systematic methods of analysis, adopted only by few authors. In this work an "integrated", multi-disciplinary approach was proposed. The analysis of geological, structural, geomorphologic and geomechanical features, by means of detailed field survey, aerial photo analysis, laboratory testing and numerical modelling, allowed to characterise kinematics, age and driving factors of the studied DSGSD case, stressing physically consistent interpretations from available data. The application of this method to a large number of cases in different lithological, structural and morphological conditions is suggested, in order to classify typologies of DSGSD by means of consistent criteria (kinematics, structural features, morpho-climatic setting).

A better comprehension of this kind of phenomena has relevant engineering geological implications. In many cases a genetic link between DSGSD and the development of large, maybe catastrophic rockslides along lower slope sectors was recognised. In fact, many large rockslides are portions of a DSGSD that have reached failure after the progressive deformation of the whole slope. Knowledge of the kinematics of a deep-seated deformation can be useful to understand the evolution of landslides and make predictions on their development.

Acknowledgements

The authors are grateful to the staff of the Servizio Geologico e Tutela dell'Ambiente of the Regione Lombardia for making available the aero-photos of the study area. The research has been funded by the MURST (Ministero per l'Università e la Ricerca Scientifica e Tecnologica). The paper benefited from the suggestions of two referees.

References

Barton, N., 1976. The shear strength of rock and rock joints. Int. J. Rock Mech. Min. Sci. Geomech. Abstr. 13, 1–24.

Barton, N.R., Choubey, V., 1977. The shear strength of rock joints in theory and practice. Rock Mech. 10 (1–2), 1–54.

Beck, A.C., 1968. Gravity faulting as a mechanism of topographic adjustment. N.Z. J. Geol. Geophys. 11 (1), 191–199.

Bieniawski, Z.T., 1989. Engineering Rock Mass Classification. Wiley, New York.

Bonsignore, G., Borgo, A., Gelati, R., Montrasio, A., Potenza, R., Pozzi, R., Ragni, U., Schiavinato, G., 1969. Note illustrative della Carta Geologica d'Italia, Foglio 8-Bormio. Servizio Geologico d'Italia, Roma.

Bovis, M.J., 1982. Uphill facing (antislope) scarps in the Coast Mountains, southwest British Columbia. Geol. Soc. Am. Bull. 93, 804–812.

Calderoni, G., Guglielmin, M., Lozej, A., Tellini, C., 1983. Research on rock glaciers in the Central Italian Alps (Valtellina, Sondrio, Northern Italy). Proceedings of the 6th International Conference on Permafrost, Bejing, China, vol. 1, pp. 72–77.

Canetta, M., Frassoni, A., Maugliani, V., Tanzini, M., 1992. Appraisal of the rock mass interested by underground excavations for the extension of a hydroelectric power plant. In: Broch, E., Lysne, D.K. (Eds.), Proceedings of the 2nd International Conference on Hydropower, Lillehammer, Norway, 16–18 June, pp. 81–88.

Catasta, G., Smiraglia, C., 1978. Il versante della Reit (bassa Valfurva). Quaderni Parco Naz Stelvio 1, 1–32.

Chigira, M., 1992. Long-term gravitational deformation of rock by mass rock creep. Engng Geol. 32 (3), 157–184.

Conti, P., 1997. La falda austroalpina dell'Ortles e l'evoluzione tettonica delle Dolomiti dell'Engadina (Svizzera-Italia). Mem. Descr. Carta Geol. d'Italia 53, 5–102.

Crosta, G., 1996. Landslide, spreading, deep seated gravitational deformation: analysis, examples, problems and proposals. Geog. Fis. Dinam. Quat. 19 (2), 297–313.

Crosta, G., Zanchi, A., 2000. Deep seated slope deformations. Huge, extraordinary, enigmatic phenomena. In: E. Bromhead

(Ed.), Proceeding of the 8th International Symposium on Landslides, Cardiff, June 2000 (in press).

Crosta, G., Agliardi, F., Frattini, P., 1999. Convenzione di studio per l'effettuazione di verifiche di stabilità e la modellazione dello scendimento delle masse rocciose potenzialmente instabili della Frana del Ruinon (Valfurva, Sondrio), nonché analisi dei dati delle reti di monitoraggio per l'individuazione di valori di soglia da utilizzare ai fini dell'allertamento. Technical report to Regione Lombardia. Dipartimento Scienze Geologiche e Geotecnologie dell'Università di Milano-Bicocca.

Cruden, D.M., Varnes, D.J., 1993. Landslides investigation and mitigation. Landslide types and processes. Transportation Research Board, National Academy of Sciences, 1–77 (Chap. 3).

Forcella, F., 1984. The Sackung between Mount Padrio and Mount Varadega, Central Alps, Italy: a remarkable example of slope gravitational tectonics. Mèditerranèe 51 (1–2), 81–92.

Forcella, F., Orombelli, G., 1984. Holocene slope deformations in Valfurva, Central Alps, Italy. Geogr. Fis. Dinam. Quat. 7, 41–48.

Forcella, F., Gallazzi, D., Montrasio, A., Notarpietro, A., 1982. Note illustrative relative all'evoluzione neotettonica dei Fogli 6 — Passo dello Spluga, 7 — Pizzo Bernina, 8 — Bormio, 17 — Chiavenna, 18 — Sondrio, 19 — Tirano. Contributi alla realizzazione della Carta Neotettonica d'Italia, Progetto Finalizzato Geodinamica, 513, 239–288.

Froitzheim, N., Schmid, S.M., Conti, P., 1994. Repeated change from crustal shortening to orogen-parallel extension in the Austroalpine units of Graubünden. Eclogae Geol. Helv. 87, 559–612.

Gregnanin, A., Valle, M., 1995. Deformation and metamorphism in Austroalpine Otztal-Stubai complex (Part I): the basement. Boll. Soc. Geol. It. 114, 373–392.

Hoek, E., Brown, E.T., 1980. Underground Excavations in Rock. Institution of Mining and Metallurgy, London (527 pp.).

Hutchinson, J.N., 1988. General report: morphological and geotechnical parameters of landslides in relation to geology and hydrogeology. Proceedings of the 5th International Symposium on Landslides, Lausanne, CH, vol. 1. Balkema, Rotterdam, pp. 3–35.

International Society for Rock Mechanics Commission on Standardisation of Laboratory and Field Tests, 1978. Suggested methods for the quantitative description of discontinuities in rock masses. Int. J. Rock Mech. Min. Sci. Geomech. Abstr. 15, 319–368.

ITASCA, 1998. FLAC (Fast Lagrangian Analysis of Continua) user's manual. ITASCA Consulting Group, Minneapolis, MN.

Jahn, A., 1964. Slopes morphological features resulting from gravitation. Zeischr. Geomorphol. Suppl. 5, 59–72.

Mahr, T., 1977. Deep-reaching gravitational deformations of high mountain slopes. IAEG Bull. 19, 121–127.

Mahr, T., Nemcok, A., 1977. Deep-seated creep deformations in the crystalline cores of the Tatry Mts. IAEG Bull. 16, 104–106.

Nemcok, A., 1972. Gravitational slope deformation in high mountains. Proceedings of the 24th International Geology Congress, Montreal, Sect. 13, pp. 132–141.

Patton, F.D., Hendron, Jr. A.J., 1974. General report on mass movements. 2nd International Congress IAEG, vol. 5, GR1–GR57.

Pelfini, M., 1987. Contributo alla conoscenza delle fluttuazioni oloceniche del Ghiacciaio dei Forni (Gruppo Ortles-Cevedale, Sondrio). "Natura bresciana". Ann. Mus. Civ. Sc. Nat. Brescia 24, 237–257.

Radbruch-Hall, D., Varnes, D.J., Colton, R.B., 1977. Gravitational spreading of steep-sided ridges ("Sackung"). Colorado J. Res. U.S. Geol. Surv. 5 (3), 359–363.

Radbruch-Hall, D., 1978. Gravitational creep of rock masses on slopes. In: Voight, B. (Ed.). Rockslides and avalanches natural phenomena. Developments in Geotechnical Engineering, vol. 14. Elsevier, Amsterdam, pp. 608–657 (Chap. 17).

Ramsay, J.C., 1967. Folding and Fracturing of Rocks. McGraw Hill, New York (568 pp.).

Savage, W.Z., Varnes, D.J., 1987. Mechanics of gravitational spreading of steep-sides ridges (sackung). IAEG Bull. 35, 31–36.

Slejko, D., Carulli, G.B., Nicolich, R., Rebez, A., Zanferrari, A., Cavallin, A., Doglioni, C., Carraro, F., Castaldini, D., Iliceto, V., Semenza, E., Zanolla, C., 1989. Seismotectonics of the Eastern-Southern Alps: a review. Boll. Geof. Teor. Appl. 31 (122), 109–136.

Smiraglia, C., 1981. Un deposito olocenico nella bassa Valfurva (Alpi Retiche). Datazione con il ^{14}C. Geogr. Fis. Dinam. Quat. 4, 102–103.

Sorriso-Valvo, M., 1995. Considerazioni sul limite tra deformazione gravitativa profonda di versante e frana. Mem. Soc. Geol. It. L, 179–185.

Stini, J., 1941. Unsere Taler Wachsen zu. Geol. Bauwes 13, 71–79.

Tabor, R.W., 1971. Origin of ridge-top depressions by large scale creep in the Olimpic Mountains. Bull. Geol. Soc. Am. 82, 1811–1822.

Ter-Stepanian, G., 1966. Type of depth creep of slopes in rock masses. Problems Geomech. 3, 49–69.

Westaway, R., 1992. Seismic moment summation for historical earthquakes in Italy: tectonic implications. J. Geophys. Res. 97 (B11), 15,437–15,464.

Zanchi, A., Gregnanin, A., Carona, P., Frassoni, A., Guida, S., 1995. Recent brittle deformation in the Central-Wetern Alps, Italy. IGCP378, circumalpine quaternary correlations. S. Alps Quat. Geol. Lugano 2-6, 1995.

Zischinsky, U., 1966. Movement of unstable valley sides. Gesellschaft der Geologic und Bergbaustudenten, Mitteil ungen 17, 127–168.

Zischinsky, U., 1969. Uber Sackungen. Rock Mech. 1 (1), 30–52.